Proceedings of the 2003 IEEE/ASME
International Conference on
Advanced Intelligent Mechatronics (AIM 2003)

A State Space Model for Modern Feedback Control of Optical Fiber Drawing Process

Serge Tchikanda
Fluid/Thermal Modeling Dept.
Sandia National Laboratories
Livermore, CA USA
swtchik@sandia.gov

Kok-Meng Lee
Mechanical Engineering Dept.
Georgia Institute of Technology
Atlanta, GA USA
kokmeng.lee@me.gatech.edu

Zhi Zhou
Fiber Draw Technology
OFS
Norcross, GA USA
zhizhou@ofsoptics.com

Abstract

Fiber diameter nonuniformities in optical fiber drawing processes can have adverse effects on system performance. In this paper we develop a method for obtaining models of the drawing process that lend themselves to the application of optimal control of fiber diameter nonuniformities. The method presented here consists of using the basic conservation laws of mass, momentum, and energy to construct state space models of the drawing process that incorporate all the relevant variables of the system in a multiple-input/multiple-output framework. An LQG optimal controller is synthesized to illustrate the applicability of the state space model.

1 INTRODUCTION

Fiber optic technology experienced a phenomenal rate of progress in the second half of the twentieth century. For the past decades, optical fibers have become an efficient and elegant way to transmit signals in many applications. The *U.S.* military uses fiber optics for improved communications and tactical systems. Computers, information networks, and data communications embraced fiber technology for a transmission system that has lighter weight cable, resists lightning strikes, and carries more information faster and over longer distances. The broadcast industry uses fiber optic video transmission system for digital video signals.

Optical fibers are manufactured by means of the draw process, which refers to the formation of an optical fiber from a cylindrical glass rod called preform. As shown in Figure 1, a preform of initial radius, R_P, is gradually fed at a rate, v_P, into a cylindrical furnace and peripherally heated to its softening temperature. At that temperature the preform becomes soft and a tension force is applied at its lower tip to pull the glass downward resulting in a necking shape on the preform. As the glass is drawn downward at a relatively high speed, v_f, a glass fiber is formed at some location downstream. When the fiber exits the furnace, it enters the cooling stage where it is cooled by the surrounding gas. The fiber is then coated with an organic material to protect its surface from moisture and direct mechanical abrasion. Finally, the coated fiber is wound on spools through a precision winding mechanism. During the drawing process, the fiber diameter may exhibit significant fluctuations due to unsteady variations of the preform feed rate, fiber draw speed, furnace temperature, and/or mechanical vibration of the drawing machine.

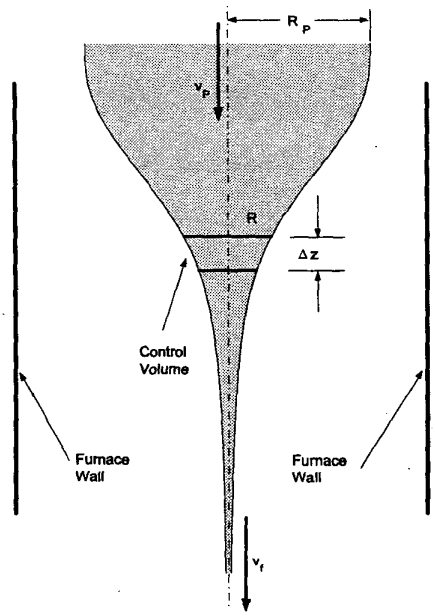

Figure 1: Longitudinal section of a typical draw process configuration

Several researchers have attempted to model the drawing process in an effort to devise better diameter controllers. Tchikanda [1] used two-dimensional fluid dynamic models to obtain the free surface shape, velocities, and temperature profiles of the glass during the drawing process. These models incorporate thousands of dynamic states and can provide accurate representations of the flow field. However, they necessitate large amount of computational time and thus, are unsuitable for both real-time simulations and control design. Mulpur and Thompson [2, 3] developed fiber diameter controllers using one-dimensional models of the draw process. Although these models require a lot less computational time than the two-dimensional ones, they are based on isothermal approximations of the full two-dimensional models and cannot be used to predict fiber diameter nonuniformities due to temperature fluctuations in the draw process. Smithgall [4] and Zhu et. al. [5] designed fiber diameter controllers

Authorized licensed use limited to: IEEE Editors in Chief. Downloaded on February 5, 2010 at 15:23 from IEEE Xplore. Restrictions apply.

based on experimentally determined frequency response models of the fiber drawing process. These frequency response models are constructed using parameter lumping methods based on the information at the boundary. Although they can accurately characterize the input/output relationship of the system, they do not reveal any information about internal states and thus, cannot predict large perturbations in the flow field like fluid dynamic models do. Furthermore, they are single-input/single-output (SISO) systems in which the draw speed is the only control input to the system. Controlling the fiber diameter using these SISO models puts a burden on the draw speed, which in turn results in large variations in draw speeds that adversely affect subsequent process operations such as the application of the coating material.

Tchikanda and Lee [6] addressed the above issues by attempting to bridge the gap between the system theoretic modeling techniques of control engineers and the more physically motivated modeling methods of fluid dynamicists. They developed a state space model that incorporates all the relevant inputs and outputs of the system in a multiple-input/multiple-output (MIMO) framework. Although their model is an improvement to the previous models, three issues are worth mentioning: 1) they do not take into account the transient behaviour of the inflow temperature. During the drawing process, the glass temperature profile is significantly affected by the inflow temperature since the latter changes drastically as the preform is lowered into the furnace. 2) They use a very high order stencil to discretize the outflow boundary. This often causes numerical instabilities of the discretization scheme and thus leads to unstable systems. 3) They use the fiber cross sectional area as one of the states instead of the fiber diameter. This practice tends to introduce very small coefficients in the system matrices, which results in ill-conditioned problems.

In this paper, the method developed in [6] is used to obtain an improved state space model that lends itself to the application of modern feedback control design techniques. Finally, a Linear Quadratic Gaussian (LQG) optimal controller is synthesized to illustrate the applicability of the state space model.

2 DYNAMIC EQUATIONS

At high temperatures, glasses used in optical fiber drawing processes are modeled as incompressible and highly viscous Newtonian liquid with temperature dependent thermophysical properties. In order to accurately capture the dynamics of such a process, the full two-dimensional conservation equations (*Navier Stokes* equations) are often used [1]. However, the complexity and computational effort required to solve these equations make them unsuitable for control design. For this reason, quasi-one-dimensional equations are used to approximate the full two-dimensional equations. This approximation is based on the fact that the flow is predominantly in the axial direction for a large portion of the drawing process especially in the draw-down region where most of the fiber formation occurs. The radial velocity component and the gradients of the velocity vector in the radial direction are small in that region. As a result, the radial momentum equation becomes negligible. The remaining equations are the continuity, axial momentum, and energy equations and describe the mean flow of glass along the axial direction. They can be obtained by applying the conservation laws of mass, momentum, and energy to an appropriate control volume. In cylindrical coordinates, a suitable control volume is an infinitesimal cylinder of diameter $d = 2R$ and length Δz as shown in Figure 1. The axial velocity and axial temperature at the center of the control volume are v and T, respectively. Hence, stated in the context of this differential control volume, the conservation of mass, momentum, and energy are given by

$$\frac{\partial}{\partial t}\left(d^2\right) + \frac{\partial}{\partial z}\left(d^2 v\right) = 0, \tag{1}$$

$$\rho\left[\frac{\partial}{\partial t}\left(d^2 v\right) + \frac{\partial}{\partial z}\left(d^2 v^2\right)\right] = \frac{\partial}{\partial z}\left[d^2\left(3\mu\frac{\partial v}{\partial z} + \kappa\gamma\right)\right] + \rho g d^2, \tag{2}$$

$$\rho c_p\left[\frac{\partial}{\partial t}\left(d^2 T\right) + \frac{\partial}{\partial z}\left(d^2 v T\right)\right] = \frac{\partial}{\partial z}\left(k d^2 \frac{\partial T}{\partial z}\right) - 4d\left(q''_{rad} + q''_{conv}\right) + d^2\left(3\mu\frac{\partial v}{\partial z} + \kappa\gamma\right)\frac{\partial v}{\partial z}, \tag{3}$$

where t is time and z is the axial distance; ρ, μ, κ, γ, and g are the density, dynamic viscosity, surface curvature, surface tension coefficient, and gravitational acceleration, respectively; c_p and k are the specific heat and thermal conductivity, respectively. The convective and radiative heat fluxes at the glass surface are given by

$$q''_{conv}(z) = h(z)\left[T(z) - T_\infty\right], \tag{4}$$

$$q''_{rad}(z,t) = \sigma\varepsilon T^4 - q(t)q''_{fur}(z), \tag{5}$$

where h is the heat transfer coefficient at the surface, T_∞ is the surrounding gas temperature, ε is the glass "*effective*" emissivity, $\sigma = 5.67051 \times 10^{-8}\,\mathrm{W\,m^{-2}\,K^{-4}}$ is the *Stefan – Boltzmann constant*, and $q(t)q''_{fur}(z)$ represents the heat flux leaving the furnace that is incident on the glass surface. The spatial distribution of the furnace heat flux, $q''_{fur}(z)$, is obtained from [1] and its intensity is given by the following differential equation:

$$\tau_q \dot{q}(t) + q(t) = K_q I_q(t), \tag{6}$$

where I_q is the input current to the furnace, and τ_q and K_q are the furnace time constant and gain, respectively.

To simplify the presentation and utilization of the solutions, the conservation equations are rewritten in dimensionless form and cast into the vector form. The nondimensionalizing procedure may be done by normalizing the relevant variables with appropriate scales and arranging them into suitable dimensionless groups.

$$d \sim D_P,\ v \sim v_f,\ z \sim L,\ t \sim L/v_f,$$
$$T \sim T_m,\ \mu \sim \mu_m,\ k \sim k_m,\ c_p \sim c_{p,m},\ \gamma \sim \gamma_m,$$

Authorized licensed use limited to: IEEE Editors in Chief. Downloaded on February 5, 2010 at 15:23 from IEEE Xplore. Restrictions apply.

where the subscript "m" denotes value at the melting point and L is the length of the drawing region. Using the above scales, the conservation equations are rewritten as

$$E\left(G\frac{\partial Q}{\partial t}+\frac{\partial F}{\partial z}\right)=\frac{\partial}{\partial z}\left(\Gamma\frac{\partial Q}{\partial z}\right)+S, \tag{7}$$

where Q, F, and S, are the state vector, convective flux vector, and source vector, respectively, given by

$$Q=\left[\begin{array}{ccc} d & v & T \end{array}\right]^T,$$
$$F=\left[\begin{array}{ccc} d^2v & d^2v^2 & d^2vT \end{array}\right]^T,$$

$$S=\left[\begin{array}{c} 0 \\ s_1\left(d^2\right)_z+d^2s_2 \\ d\left\{s_5T^4+s_6q(t)q''_{fur}(z)+s_7\left(T-T_{\infty,m}\right)\right\} \\ +d^2\left(s_3v_z^2+s_4v_z\right) \end{array}\right],$$

where

$$s_1=\frac{\kappa\gamma}{ReCa},\ s_2=\frac{\partial s_1}{\partial z}+\frac{1}{Fr},\ s_3=\frac{3\mu Ec}{Re},\ s_4=s_1Ec,$$

$$s_5=-\frac{4L\sigma\varepsilon T_m^3}{\rho v_f c_{p,m}D_P},\ s_6=\frac{4L/D_P}{\rho v_f T_m c_{p,m}},\ s_7=-\frac{4Lh/D_P}{\rho v_f c_{p,m}}.$$

The matrices E, G, and Γ are given by

$$E=diag\left(1,1,c_p\right),\ G=\left[\begin{array}{ccc} 2d & 0 & 0 \\ 2dv & d^2 & 0 \\ 2dT & 0 & d^2 \end{array}\right],$$
$$\Gamma=diag\left(0,\frac{3\mu d^2}{Re},\frac{kd^2}{Pe}\right).$$

The dimensionless groups Re, Pe, Fr, Ec, and Ca are the *Reynolds*, *Peclet*, *Froude*, *Eckert*, and *Capillary* numbers, respectively, defined by

$$Re=\frac{\rho v_f L}{\mu_m},\ Pe=\frac{v_f L}{k_m/\rho c_{p,m}},\ Fr=\frac{v_f^2}{gL},$$
$$Ec=\frac{v_f^2}{c_{p,m}T_m},\ Ca=\frac{\mu_m v_f}{\gamma_m},\ T_{\infty,m}=\frac{T_\infty}{T_m}.$$

3 BOUNDARY CONDITIONS

The preform diameter is constant at the inflow boundary and is equal to $D_P=2R_P$. At the outflow, the equation for the fiber diameter is obtained by spatially discretizing the continuity equation given by Eq. (1) using one-sided differences.

The axial velocity at the inflow is equal to the preform feed rate, $v_P(t)$, which is obtained from a motor described by

$$\tau_P\dot{v}_P\left(t\right)+v_P\left(t\right)=K_PV_P(t), \tag{8}$$

where V_P is the input voltage to the motor, and τ_P and K_P are the motor time constant and gain, respectively. Similarly, the outflow velocity is equal to the fiber draw speed, $v_f(t)$, obtained from a motor described by

$$\tau_f\dot{v}_f\left(t\right)+v_f\left(t\right)=K_fV_f(t), \tag{9}$$

where V_f is the input voltage to the motor, and τ_f and K_f are the motor time constant and gain, respectively.

For high speed drawing of long fibers, conduction heat transfer is negligible at the inflow and outflow boundaries. As a result, only the advection, convection, and radiation terms are retained in the energy equation. Thus, at the inflow and outflow boundaries the first and last terms on the right in Eq. (3) can be dropped leading to the following dimensionless equation

$$c_p\left[\frac{\partial}{\partial t}\left(d^2T\right)+\frac{\partial}{\partial z}\left(d^2vT\right)\right]=$$
$$d\left[s_5T^4+s_6q(t)q''_{fur}(z)+s_7\left(T-T_{\infty,m}\right)\right]. \tag{10}$$

Eq. (10) will be spatially discretized using one-sided differences to obtain equations for the inflow and outflow temperatures.

4 STATE SPACE MODEL

The conservation equations developed in the previous sections emphasized the fact that instabilities in the draw process are due to unsteady dynamics of the diameter, velocity, and temperature profiles. The framework for analyzing these instabilities is based on the conservation of mass, momentum, and energy. In this section, a state space form suitable for the application of modern control design techniques is introduced. This is achieved by linearizing and spatially discretizing the conservation equations, which are rewritten here as

$$N\frac{\partial Q}{\partial t}=\mathcal{R}\left(Q,q\right), \tag{11}$$

where the residual vector, $\mathcal{R}$, is defined as

$$\mathcal{R}\equiv\frac{\partial}{\partial\xi}\left(\Gamma\frac{\partial Q}{\partial\xi}\right)-E\frac{\partial F}{\partial\xi}+S, \tag{12}$$

and the matrix $N=EG$.

In order to discretize the conservation equations, a one-dimensional grid along the axial coordinate is constructed on the solution domain. The grid points are numbered using the index i with $1\le i\le I$, where I is the maximum number of grid points. The inflow boundary is located at $i=1$ whereas the outflow is at $i=I$. The residual vector is discretized using a third order upwind flux difference method [7] for the convective flux vector, and the second order central difference method [8] for the diffusion term and source term vector. Thus,

$$\mathcal{R}_i\approx\Gamma_{i+1/2}\left(Q_{i+1}-Q_i\right)-\Gamma_{i-1/2}\left(Q_i-Q_{i-1}\right)$$
$$+\frac{1}{3}E_i\left[\Omega_{i+1/2}\left(Q_{i+1}-Q_i\right)-\Omega_{i-1/2}\left(Q_i-Q_{i-1}\right)\right]$$
$$-\frac{1}{2}E_i\left[F\left(Q_{i+1}\right)-F\left(Q_{i-1}\right)\right]+S_i. \tag{13}$$

Authorized licensed use limited to: IEEE Editors in Chief. Downloaded on February 5, 2010 at 15:23 from IEEE Xplore. Restrictions apply.

where $\Omega = \partial F/\partial Q$ is the *Jacobian* matrix of the convective flux vector. The discrete residual vector in Eq. (13) can be linearized using a truncated *Taylor* series about some steady state vector, Q, and heat flux, q, to give

$$N_i \delta \dot{Q}_i = \alpha_i \delta Q_{i-1} + \beta_i \delta Q_i + \varphi_i \delta Q_{i+1} + \omega_i \delta q, \qquad (14)$$

where δQ and δq are small perturbations about some steady state, and the coefficient matrices are given by

$$\alpha_i = \frac{\partial \mathcal{R}_i}{\partial Q_{i-1}},\ \beta_i = \frac{\partial \mathcal{R}_i}{\partial Q_i},\ \varphi_i = \frac{\partial \mathcal{R}_i}{\partial Q_{i+1}},\ \omega_i = \frac{\partial S_i}{\partial q}.$$

As mentioned in the previous section, the diameter at the inflow is constant ($d_1 = D_P$). Therefore the inflow state vector, Q_1, has only two components, v_1 and T_1 given by Eqs. (8) and (10), respectively. The outflow equation for the state vector $Q_I = [d_I\ v_I\ T_I]^T$ is obtained using Eqs. (1), (9), and (10) for d_I, v_I, and T_I, respectively, with one-sided differences used when appropriate.

Combining Eqs. (6), (8), (9) and (14) along with the discretized versions of Eqs. (1) and (10) at the inflow and outflow boundaries, the system state equation can be rewritten as

$$M\dot{x}(t) = A_1 x(t) + B_1 u(t), \quad t \in [0, \infty), \qquad (15)$$

where the state vector x and the input vector u are

$$x = \left[\ \delta q \quad \delta Q_1 \quad \delta Q_2^T \quad \cdots \quad \delta Q_i^T \quad \cdots \quad \delta Q_I^T\ \right]^T,$$
$$u = \left[\ V_P \quad V_f \quad I_q\ \right]^T.$$

The matrices M, A_1, and B_1 are given by

$$M = \textit{block-diag}\,(\tau_q, N_1, N_2, \cdots, N_i, \cdots, N_I),$$

$$A_1 = \begin{bmatrix} \beta_1 & \varphi_1 & & & & & \\ \alpha_2 & \beta_2 & \varphi_2 & & & & \\ \overline{\omega}_3 & \alpha_3 & \beta_3 & \varphi_3 & & & \\ & \ddots & \ddots & \ddots & & & \\ \overline{\omega}_i & & \alpha_i & \beta_i & \varphi_i & & \\ \vdots & & & \ddots & \ddots & \ddots & \\ \vdots & & & & \alpha_{I-1} & \beta_{I-1} & \varphi_{I-1} \\ \overline{\omega}_I & & & & & \alpha_I & \beta_I \end{bmatrix},$$

$$B_1 = \left[\ B_{11}^T \quad 0_{3\times(I-6)} \quad B_{1I}^T\ \right]^T,$$

where $\overline{\omega}_i = [\omega_i\ 0_{3\times 2}]$ and

$$B_{11} = \begin{bmatrix} 0 & 0 & K_q \\ K_P & 0 & 0 \\ 0 & 0 & 0 \end{bmatrix},\ B_{1I} = \begin{bmatrix} 0 & 0 & 0 \\ 0 & K_f & 0 \\ 0 & 0 & 0 \end{bmatrix}.$$

Eq. (15) is the linear state-variable form of the dynamic equations. To complete the state space representation of the system, an output equation must be developed. The outputs of the system are the fiber diameter and the fiber tension force. In dimensionless form, the fiber tension force is given by

$$f = d^2\left(3\mu\frac{\partial v}{\partial z} + \frac{\kappa\gamma}{Ca}\right). \qquad (16)$$

Using a second-order backward difference for the velocity gradient at the outflow boundary[1], Eq. (16) is discretized and linearized to give

$$\delta f_I = c_1 \delta Q_I + c_2 \delta Q_{I-1} + c_3 \delta Q_{I-2}, \qquad (17)$$

where the vectors c_1, c_2, and c_3 are obtained in an obvious manner. Denoting the output vector by

$$y = \left[\ \delta d_I \quad \delta f_I\ \right]^T,$$

the complete state space representation of the dynamic system is expressed as

$$\dot{x}(t) = Ax(t) + Bu(t), \quad t \in [0, \infty), \qquad (18)$$
$$y(t) = Cx(t) + Du(t), \qquad (19)$$

where

$$A = M^{-1}A_1,\ B = M^{-1}B_1,\ D = 0_{2\times 3}$$
$$C = \begin{bmatrix} 0_{1\times 3} & \cdots & 0_{1\times 3} & \cdots & 0_{1\times 3} & e_1 \\ 0_{1\times 3} & \cdots & 0_{1\times 3} & c_3 & c_2 & c_1 \end{bmatrix}.$$

and $x \in \Re^{n\times 1}$, $u \in \Re^{3\times 1}$, $y \in \Re^{2\times 1}$, $A \in \Re^{n\times n}$, $B \in \Re^{n\times 2}$, $C \in \Re^{2\times n}$, $D \in \Re^{2\times 3}$, $e_1 = \left[\ 1 \quad 0 \quad 0\ \right]$, and $n = 3I$.

5 CONTROL DESIGN

In this section, an *LQG* optimal controller is synthesized to illustrate the applicability of the state space model developed in the previous section. The control objective is to minimize the unsteady fluctuations in fiber diameter and tension force due to a disturbance input in furnace heat flux which may arise from furnace temperature fluctuations. For controller synthesis a disturbance noise source is introduce on the furnace and sensors noise are included in the model. The design plant model is hence given by

$$\dot{x}(t) = Ax(t) + Bu(t) + D_1 w(t), \quad t \in [0, \infty), \qquad (20)$$
$$y(t) = Cx(t) + Du(t) + D_2 w(t), \qquad (21)$$

where D_1 is given by

$$D_1 = \begin{bmatrix} 0 & \sigma_1 \omega_1^T N_1^{-T} & \cdots & \sigma_I \omega_I^T N_1^{-T} \\ 0 & 0_{2\times 2} & \cdots & 0_{2\times 3} \end{bmatrix}^T,$$

where $\sigma_1, \ldots, \sigma_I$ are weights that can be chosen as design parameters,

$$D_2 = \begin{bmatrix} 0 & D_{21} & 0 \\ 0 & 0 & D_{22} \end{bmatrix},$$

is the weighting on the fiber diameter and tension force sensors noise, and $w(t) = \left[\ w_1(t) \quad w_2(t) \quad w_3(t)\ \right]^T$. The signals $w_1(t)$, $w_2(t)$, and $w_3(t)$ represent the furnace disturbance noise, fiber diameter sensor noise, and fiber tension force sensor noise, respectively, and are assumed to

[1] It is assumed that the final fiber diameter is attained at the outflow boundary and the tension force is measured there.

Authorized licensed use limited to: IEEE Editors in Chief. Downloaded on February 5, 2010 at 15:23 from IEEE Xplore. Restrictions apply.

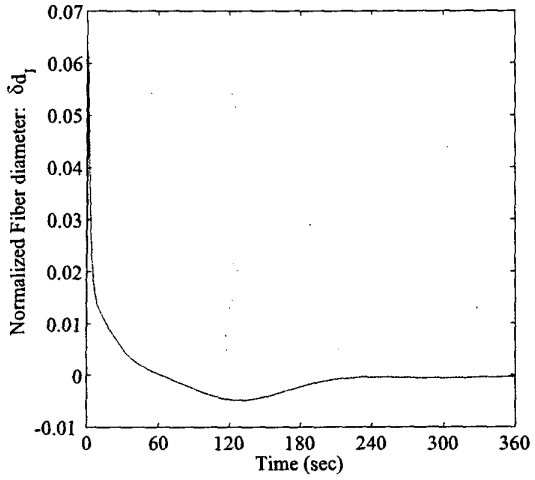

Figure 2: Fiber diameter closed-loop free response of LQG controller.

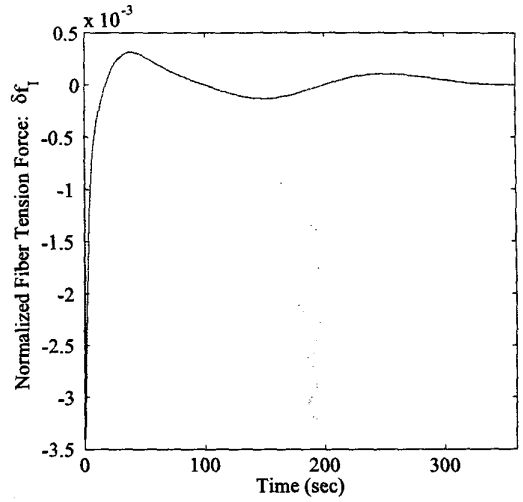

Figure 3: Fiber tension force closed-loop free response of LQG controller.

be uncorrelated unit-intensity white noise processes. The performance variable

$$\xi(t) = E_1 x(t) + E_2 u(t), \tag{22}$$

consists of a weighted sum of the state variables and control signals. Since the control objective is to minimize the unsteady fluctuations in fiber diameter and tension force, the performance state matrix E_1 has the same form as the output matrix C and is thus given by

$$E_1 = \begin{bmatrix} 0_{1\times3} & \cdots & 0_{1\times3} & \cdots & 0_{1\times3} & \lambda_1 e_1 \\ 0_{1\times3} & \cdots & 0_{1\times3} & \lambda_2 c_3 & \lambda_2 c_2 & \lambda_2 c_1 \\ 0_{3\times3} & \cdots & 0_{3\times3} & \cdots & 0_{3\times3} & 0_{3\times3} \end{bmatrix},$$

where λ_1 and λ_2 are weights that can be chosen as design parameters. The control weighting matrix is given by

$$E_2 = \begin{bmatrix} 0 & 0 & E_{21} & 0 & 0 \\ 0 & 0 & 0 & E_{22} & 0 \\ 0 & 0 & 0 & 0 & E_{23} \end{bmatrix}^T.$$

The performance consideration of the LQG problem is to minimize the H_2 norm of the closed-loop system from disturbance variable $w(t)$ to performance variable $\xi(t)$. Hence, using the framework presented in [9] we design a dynamic compensator of order $n_c = n$ of the form

$$\dot{x}_c(t) = A_c x_c(t) + B_c y(t), \quad t \in [0, \infty), \tag{23}$$
$$u(t) = C_c x(t), \tag{24}$$

such that the closed-loop system Eqs. (20), (21), (23), and (24) given by

$$\dot{\widetilde{x}}(t) = \widetilde{A}\widetilde{x}(t) + \widetilde{D}w(t), \quad t \in [0, \infty), \tag{25}$$
$$\xi(t) = \widetilde{E}\widetilde{x}(t), \tag{26}$$

where

$$\widetilde{x} = \begin{bmatrix} x(t) \\ x_c(t) \end{bmatrix}, \quad \widetilde{A} = \begin{bmatrix} A & BC_c \\ B_c C & A_c \end{bmatrix},$$
$$\widetilde{D} = \begin{bmatrix} D_1 \\ B_c D_2 \end{bmatrix}, \quad \widetilde{E} = \begin{bmatrix} E_1 & E_2 C_c \end{bmatrix},$$

is asymptotically stable and the steady state performance criterion

$$J(A_c, B_c, C_c) = \lim_{t\to\infty} \frac{1}{t} \mathsf{E} \int_0^t \xi^T(s)\xi(s)ds, \tag{27}$$

where E denotes expectation, is minimized.

Using the above framework, an LQG controller was designed to control fiber diameter and tension force fluctuations in optical fiber drawing process. The number of grid points was $I = 50$ and all parameters such as preform shape, furnace configuration, thermophysical properties, and dimensionless groups were all obtained from [1] and will not be reproduced here due to lack of space. The steady state operating points used in the linearization procedure were obtained from nonlinear simulations [1]. Figures 2 and 3 show the LQG control free responses and Figures 4 to 6 show the LQG control input signals.

6 CONCLUSION

The objective of this paper has been to develop the dynamic equations for optical fiber drawing in a form that is accessible to control systems designers requiring state space models for modern optimal control design. Using the preform feed rate, fiber draw speed, and furnace heat input, an LQG controller was designed to actively control the unsteady fluctuations in fiber diameter and tension force. The design example illustrates the applicability of state space models in optical fiber drawing for designing modern optimal controllers.

The results of this paper can be readily extended in several directions. Specifically, since all nominal models are subject to uncertainties in the system due to unmodeled dynamics and/or inaccurate knowledge of the system parameters, it is important that the model uncertainty structure be accounted for in the control system design process.

Authorized licensed use limited to: IEEE Editors in Chief. Downloaded on February 5, 2010 at 15:23 from IEEE Xplore. Restrictions apply.

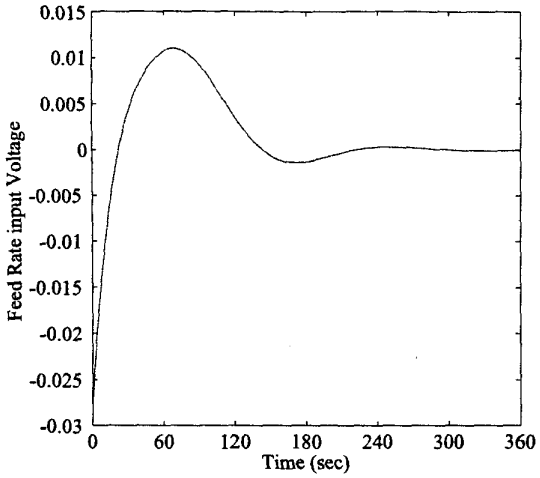

Figure 4: Feed rate control signal of LQG controller.

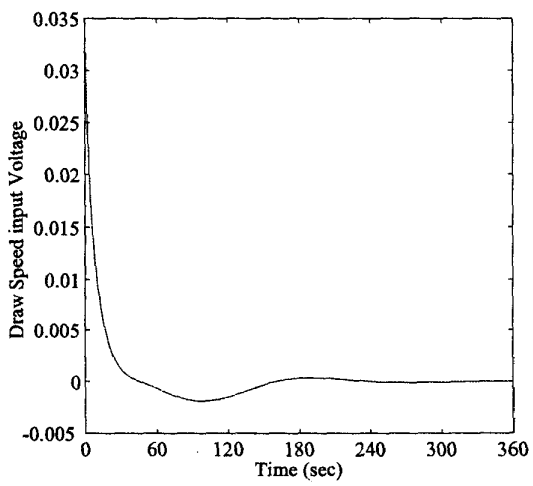

Figure 5: Draw speed control signal of LQG controller.

Particularly, in order to guarantee that the compensators designed on the basis of plant nominal dynamics or nominal models will result in stable feedback control system, the control engineer must be equipped with models that capture the uncertainty structure of the system.

ACKNOWLEDGEMENTS

This work was performed while the first author was a Ph.D student at the Georgia Institute of Technology and was sponsored by Lucent Technologies, Norcross GA. The authors would like to thank Dr. Siu-Ping Hong of OFS for his technical input and financial support.

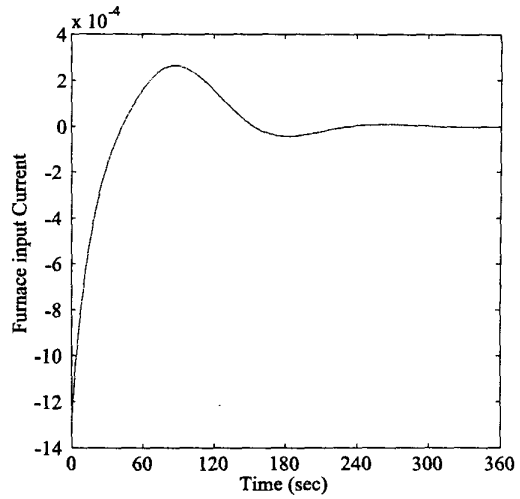

Figure 6: Furnace control signal of LQG controller.

REFERENCES

[1] S. W. Tchikanda, *Modeling for High-Speed High-Strength Precision Optical Fiber Drawing.* PhD thesis, The Georgia Institute of Technology, May 2001.

[2] A. Mulpur and C. Thompson, "Modal diameter control of linear isothermal optical fibers," in *Second IEEE Conference on Control Applications*, (Vancouver, B.C.), p. 433, September 1993.

[3] A. Mulpur and C. Thompson, "Nonlinear control of optical fiber diameter variations," in *Proceedings of the American Control Conference*, (Baltimore MD), p. 3528, June 1994.

[4] D. M. Smithgall, "Application of optimization theory to the control of the optical fiber drawing process," *Bell Sys. Tech. J.*, vol. 58, no. 6, p. 1425, 1979.

[5] Z. Zhu, G. Dai, and T. Yu, "An optical fiber drawing self-tuning control system," in *Proceedings of the IFAC/IFORS Symposium on Identification and System Parameter Estimation*, (Beijing), p. 1291, 1988.

[6] S. W. Tchikanda and K. M. Lee, "State space modeling for optical fiber drawing process," in *Proceedings of the American Control Conferencce*, (Anchorage AK), pp. 4954–4959, May 2002.

[7] S. E. Rogers and D. Kwak, "Upwind differencing scheme for the time-accurate incompressible navier-stokes equations," *AIAA Journal*, vol. 28, pp. 253–262, February 1990.

[8] J. C. Tannehill, D. A. Anderson, and R. H. Pletcher, *Computational Fluid Mechanics and Heat Transfer.* Taylor Francis, 2nd ed., 1997.

[9] D. S. Bernstein and W. M. Haddad, "Control-system synthesis: The fixed-structure approach." Georgia Tech Bookstore, March 1995.

Authorized licensed use limited to: IEEE Editors in Chief. Downloaded on February 5, 2010 at 15:23 from IEEE Xplore. Restrictions apply.